Pyrrolidine dithiocarbamate sensitizes U251 brain glioma cells to temozolomide via downregulation of *MGMT* and *BCL-XL*

JUN-HAI TANG[1], GUO-HAO HUANG[1], KE-JIE MOU[1], ERIC ERQUAN ZHANG[2], NINGNING LI[3], LEI DU[1], XIAO-PENG ZHU[1], LING CHEN[4], HUI YANG[1], KE-BIN ZHANG[5] and SHENG-QING LV[1]

[1]Department of Neurosurgery, Xinqiao Hospital, Third Military Medical University, Chongqing 400037; [2]National Institute of Biological Sciences, Beijing 102206, P.R. China; [3]Division of Neuropathology and Department of Neurodegenerative Disease, Institute of Neurology, University College London, London WC1N 3BG, UK; [4]Department of Neurosurgery, Chinese PLA General Hospital, Beijing 100853; [5]Central Laboratory, Xinqiao Hospital, Third Military Medical University, Chongqing 400037, P.R. China

Received November 21, 2015; Accepted December 16, 2016

DOI: 10.3892/ol.2017.6849

Abstract. The current study investigated the effect of pyrrolidine dithiocarbamate (PDTC) on the proliferation, apoptosis, cell cycle and sensitivity to temozolomide (TMZ) of the U251 glioma cell line. Proliferation, apoptosis and cell cycle analysis of U251 cells following treatment with PDTC and TMZ was determined by an MTT assay and flow cytometry, respectively. The mRNA and protein expression levels of O-6-methylguanine-DNA methyltransferase (*MGMT*), B-cell lymphoma extra-large *(BCL-XL)* and *survivin* were further determined by reverse transcription-quantitative polymerase chain reaction (RT-qPCR) and western blotting analysis. The results revealed that treatment with TMZ, PDTC and TMZ + PDTC significantly inhibited cell proliferation, induced apoptosis and contributed to cell cycle arrest in U251 cells. A combination of PDTC and TMZ induced the highest rates of proliferation inhibition and apoptosis. PDTC treatment markedly reduced the expression levels of *MGMT*, *BCL-XL* and *survivin*. The expression levels of *MGMT* and *BCL-XL*, were significantly upregulated by TMZ but not by combination treatment of TMZ and PDTC. The results of the present study suggest that treatment with PDTC inhibits cell proliferation, induces apoptosis and cell cycle arrest, and enhances sensitivity to TMZ in U251 cells, which is partly induced by downregulation of *MGMT* and *BCL-XL*.

Correspondence to: Professor Sheng-Qing Lv, Department of Neurosurgery, Xinqiao Hospital, Third Military Medical University, 183 Xinqiao Street, Shapingba, Chongqing 400037, P.R. China
E-mail: lvsq0518@hotmail.com

Professor Ke-Bin Zhang, Central Laboratory, Xinqiao Hospital, Third Military Medical University, 183 Xinqiao Street, Shapingba, Chongqing 400037, P.R. China
E-mail: zhangkebin12@163.com

Key words: pyrrolidine dithiocarbamate, brain glioma, nuclear factor-κB, O-6-methylguanine-DNA methyltransferase, temozolomide

Introduction

Brain glioma is the most common type of primary tumor in the central nervous system and is one of the leading causes of mortality in patients with cancer (1,2). Currently an integrated therapeutic method of surgery, radiotherapy and chemotherapy has been adopted in clinical high-grade glioma treatment (3). Patients receiving radiotherapy with concomitant and adjuvant temozolomide (TMZ), demonstrated certain advances in progression-free survival (PFS) and 5-year survival; however, the rate of total survival has not improved (4). TMZ is an oral administered alkylating chemotherapeutic drug, capable of crossing the blood-brain barrier and has been widely used to treat refractory anaplastic astrocytoma and newly diagnosed glioblastoma multiforme (5,6). The therapeutic benefits of TMZ treatment primarily depend on its ability to methylate the O-6 positions of guanine residues (7). This methylation induces irreversible damage to the DNA and triggers abnormal activation of the repair system, leading to cycle arrest and cell death (7). However, certain tumor cells are able to repair this type of DNA damage by expression of the protein, O6-alkylguanine DNA alkyltransferase (AGT), encoded in humans by the O-6-methylguanine-DNA methyltransferase (*MGMT*) gene (8). A previous study revealed that the presence of MGMT protein diminishes the therapeutic efficacy of TMZ in brain tumors; the study also indicated that high *MGMT* expression predicts poor response to TMZ and little benefit from chemotherapy with TMZ (9). Conversely, in specific cases, suppressed synthesis of MGMT due to methylation of the *MGMT* gene promoter is considered a good prognostic factor in TMZ treated patients with glioma (10). At the molecular level, several mechanisms, including nuclear factor-κB (NF-κB) (11), tumor protein 53 (12), specificity protein 1 (12), clone of myelocytomatosis viral oncogene in cancer (Myc) (13) and c-Jun N-terminal kinase (JNK) (14) mediated signaling pathways, have been suggested to be involved in the transcription regulation of *MGMT*. As a consequence, modifying

MGMT expression via its transcription factors has been proposed as a means to sensitize tumor cells to TMZ (15).

NF-κB represents a family of ubiquitous transcription factors that modulate the expression levels of genes by binding to specific κB sites (16). The activity of NF-κB is regulated by the NF-κB inhibitory protein (IκB) (17). In the inactive state, IκB binds to and sequesters NF-κB family members in the cytoplasm (17). Following NF-κB signaling pathway activation by various stimuli, including hypoxia, cytokines and chemotherapeutic drugs, IκB is phosphorylated by IκB kinase (IKK) (17); phosphorylated IκB is subjected to ubiquitination and kinase proteasome-mediated degradation, which results in the activation and translocation of NF-κB to the nucleus (17). Excluding its roles in innate immunity and inflammation, the NF-κB signaling pathway was revealed to regulate a number of cellular processes, including cell proliferation, differentiation and apoptosis (16-18). Furthermore, it has been reported that activation of the NF-κB signaling pathway may also contribute to tumor initiation, progression and resistance to radiotherapy or chemotherapy (19,20). High constitutive NF-κB activity has been observed in numerous lymphoid and myeloid tumors (21), in addition to various solid tumors, including pancreatic cancer (22), glioblastoma (23) and breast cancer (24). Certain recent studies demonstrated that hypoxia may activate the NF-κB signaling pathway, induce the epithelial-mesenchymal transition of breast cancer cells (24), cause invasion of pancreatic cancer cells and contribute to gemcitabine mediated resistance (25).

The present study focused on the association between NF-κB activity and glioma cell progression and chemotherapy. The critical roles which NF-κB serves in the progression and chemoresistance of gliomas have been demonstrated by accumulating experimental evidence (26). Similar to *MGMT*, NF-κB also contributes to the development of glioma resistance to alkylating agents (27). Furthermore, certain studies indicated that NF-κB associated chemoresistance was partially mediated by the NF-κB/*MGMT* signaling pathway, which may be activated by alkylating drugs (28,29). In order to determine the effect of inhibiting NF-κB activity on glioma cell viability and sensitivity to alkylating drugs, in addition to clarifying the underlying molecular mechanisms, the present study compared the proliferation inhibiting, cell apoptosis inducing and cell cycle arresting effects of TMZ, pyrrolidine dithiocarbamate (PDTC) and TMZ + PDTC combined. This was followed by determining the expression level alterations of *MGMT* and other associated genes, including B-cell lymphoma extra large (*BCL-XL*) and *survivin*. The present study aimed to further current understanding of the effects and the underlying molecular mechanisms of inhibiting NF-κB activity in glioma therapy, and aid the development of a clinical strategy with combined TMZ and NF-κB inhibitors.

Materials and methods

Chemicals and reagents. Dulbecco's modified Eagle's medium (DMEM), fetal bovine serum (FBS) and TRIzol® were obtained from Invitrogen (Thermo Fisher Scientific, Inc., Waltham, MA, USA); temozolomide and dimethyl sulfoxide (DMSO) were purchased from Sigma Aldrich (Merck Millipore, Darmstadt, Germany); the MTT, cell cycle and apoptosis analysis kit, Annexin V-fluorescein isothiocyanate (FITC) kit, Bradford protein assay kit, radioimmunoprecipitation assay, lysis buffer, phenyl methanesulfonyl fluoride and BeyoECL Plus were all purchased from Beyotime Institute of Biotechnology (Haimen, China). A Prime Script™ RT Master Mix was obtained from Takara Bio, Inc. (Otsu, Japan); a KAPA SYBR Fast qPCR kit was purchased from Kapa Biosystems, Inc. (Wilmington, MA, USA). The primary antibodies used for western blot analysis were mouse anti *MGMT*, *BCL-XL*, *survivin* and β-actin, and the secondary antibodies used were horseradish peroxidase-conjugated goat anti-mouse IgG (H + L), all supplied by Abcam (Cambridge, UK).

Cell lines and cell culture. The U251 human glioblastoma cell line was purchased from the National Institute of Biological Sciences (Beijing, China) and cultured in DMEM (DMEM basic 1X 1199500) supplemented with 10% FBS (10099141) (both from Gibco; Thermo Fisher Scientific, Inc.). Cells were incubated for about 6 months at 37˚C in a humidified chamber with 5% CO_2.

MTT assays for cell proliferation. Exponentially growing U251 cells were digested and re-plated into 96-well plates ($4x10^3$ cells; 100 μl/well; six repeat wells in each column). These plates were randomly divided into four groups: TMZ group, PDTC group, TMZ + PDTC group and control group. Following an incubation of 24 h, the groups were cultured as follows: Medium of the TMZ group was replaced with fresh medium (DMEM basic 1X with 10% FBS) containing 200 μmol/l TMZ; PDTC group was divided into three subgroups and medium of the three subgroups were replaced with fresh medium (DMEM basic 1X with 10% FBS) containing 20, 50 and 80 μmol/l PDTC; TMZ + PDTC group was divided into three groups and medium of the three subgroups were replaced with fresh medium (DMEM basic 1X with 10% FBS) containing 200 μmol/l TMZ and 20 μmol/l PDTC, 200 μmol/l TMZ and 50 μmol/l PDTC or 200 μmol/l TMZ and 80 μmol/l PDTC. DMSO was added into the control group. A column from each group was evaluated every 24 h and 10 μl/well MTT (5 mg/ml) was added to six wells in one column. Following incubation for 4 h, 100 μl/well formazan solution was added and incubated for an additional 4 h. Absorbance was determined at 570 nm, using an Ultra multi-functional microplate reader (Tecan Group, Ltd., Durham, NC, USA). The evaluation was performed for five consecutive days and the cell inhibition rates were calculated as follows: Rate of proliferation inhibition = [mean optical density (OD) value of control cells - mean OD value of treated cells]/mean OD value of control cells. The results were confirmed by ≥3 repetitions.

Flow cytometry detecting cell apoptosis and cell cycle distribution. U251 cells ($8x10^5$) were re-plated in 6-well plates (9.6 cm^2). Fresh medium (DMEM basic 1X with 10% FBS) was added with the following supplements: 200 μmol/l TMZ into the TMZ group; 20 μmol/l PDTC, 50 μmol/l PDTC and 80 μmol/l PDTC into the three subgroups of the PDTC group, respectively; 200 μmol/l TMZ and 20 μmol/l PDTC, 200 μmol/l TMZ and 50 μmol/l PDTC or 200 μmol/l TMZ and 80 μmol/l PDTC, into the three subgroups of the TMZ + PDTC group, respectively; 200 μmol/l TMZ and 100 μmol/l PDTC

Table I. Reaction system and conditions for RT-qPCR analysis.

Reaction system		Reaction conditions	
Reagents	Amount added, μl	Step	Action
2X KAPA SYBR Fast qPCR Master Mix Universal	7.50	1.	95˚C for 2 min
10 μM forward primer	0.15	2.	95˚C for 5 sec
10 μM reverse primer	0.15	3.	60˚C for 20 sec, value read
cDNA template	1.00 (50.00 ng)	4.	Repeat 2 and 3 for 39 repetitions
PCR-grade water	6.20	5.	Melt curve 65˚C to 95˚C in increments of 0.5˚C, for 5 sec each, value read, end.

RT-qPCR, reverse transcription-quantitative polymerase chain reaction.

into the fourth subgroup of the TMZ + PDTC group (only added in this part of the experiment); and the solvent DMSO was added into control group. Following incubation for 24 h, cells were digested by trypsinization and detached cells in the medium were collected. Cells were harvested and washed with cold PBS, $5x10^5$ cells were collected in 1.5 ml microtubes (MCT-150-C; Axygen, Union City, CA, USA). Subsequently, cells were gently resuspended in 100 μl 1X binding buffer with 5 μl Annexin V-FITC and 5 μl propidium iodide (PI) staining solution. Following incubation for 15 min in the dark at 25˚C, cells were mixed gently with 400 μl 1X binding buffer and filtered with a 0.45 μm filter unit Millex-HV (Merck Millipore), prior to flow cytometry analysis (FACSCalibur™; BD Biosciences, San Jose, CA, USA). Subsequent analyses of flow cytometry data were performed using CellQuest Pro software (version 5.1; BD Biosciences). For cell cycle distribution evaluation, cells (groups with 100 μmol/l PDTC were removed) were collected and resuspended with cold ethanol (70%) and fixed in ethanol for 12 h at 4˚C, prior to being harvested. Following washing with cold PBS twice, cells were mixed gently with 500 μl PI and incubated for 30 min in the dark at 35˚C. Cell cycle distribution was detected using flow cytometry.

Reverse transcription-quantitative polymerase chain reaction (RT-qPCR) analysis. Cells ($5x10^6$ cells initially seeded) were cultured in 6-well plates and the following treatment was administered for 48 h at 37˚C, in a humidified chamber containing 5% CO_2: 80 μmol/l PDTC to the PDTC group, 200 μmol/l TMZ to the TMZ group, 200 μmol/l TMZ and 50 μmol/l PDTC to the TMZ + PDTC group, and DMSO to the control groups. Total RNA was extracted using TRIzol® reagent, according to the manufacturer's instructions. First-strand cDNA was reverse transcribed from 1 mg total RNA using the Prime Script™ RT Master Mix, and target gene mRNA was amplified by the KAPA SYBR Fast qPCR kit, using a Bio-Rad CFX96™ real-time system (Bio-Rad Laboratories, Inc., Hercules, CA, USA). The reaction system (15 μl), PCR conditions and gene specific primers are presented in Tables I and II.

Western blot analysis. Cells were cultured in 6-cm dishes, following grouping and treatment as in RT-qPCR analysis; the cell lysates were harvested and protein level was evaluated using Bradford Protein Assay kit (P0006C; Beyotime Institute of Biotechnology). Equal amounts of total protein (80-200 μg) were separated using 10% SDS-PAGE and transferred to polyvinylidene difluoride membranes. Subsequent to blocking with 5% fat-free milk and 0.1% Tween-20 in PBS-T for 1 h at room temperature, the membranes were incubated with a dilution of anti-*MGMT* (mouse monoclonal MT3.1 to MGMT; ab39253; 1:500), anti-*BCL-XL* (mouse monoclonal MT3.1 to MGMT; ab39253; 1:500), anti-*survivin* (mouse monoclonal 60.11 to survivin; ab93274; 1:800) and anti-β-actin (anti-β-actin antibody mAbcam 8226, ab8226; 1:600) (all from Abcam) primary antibodies. Horseradish peroxidase-conjugated anti-mouse secondary antibodies (goat anti-mouse IgG H&L horseradish peroxidase pre-adsorbed; ab97040; 1:1200; Abcam) were used, and bound antibodies were detected using the BeyoECL system (P0018; Beyotime Institute of Biotechnology).

Statistical analysis. Data are presented as the mean ± standard deviation. All statistical analyses were performed using SPSS 13.0 software (SPSS, Inc., Chicago, IL, USA). The Student's t-test (one sample or independent-samples t-test) was used to analyze the difference between the means of the treatment group and the control group. One-way analysis of

Table II. Gene primers for RT-qPCR analysis.

Gene	Primer
MGMT	F: 5'-GGGTCTGCACGAAATAAAGC-3' R: 5'-CTCCGGACCTCCGAGAAC-3'
BCL-XL	F: 5'-AAAAGATCTTCCGGGGGCTG-3' R: 5'-CCCGGTTGCTCTGAGACATT-3'
Survivin	F: 5'-TTCTCAAGGACCACCGCATC-3' R: 5'-AATGGGGTCGTCATCTGGCT-3'
β-actin	F: 5'-GTACCACTGGCATCGTGATGGACT-3' R:5'-ATCCACACGGAGTACTTGCGCTCA-3'

MGMT, O-6-methylguanine-DNA methyltransferase; BCL-XL, B-cell lymphoma extra-large; RT-qPCR, reverse transcription-quantitative polymerase chain reaction; F, forward; R, reverse.

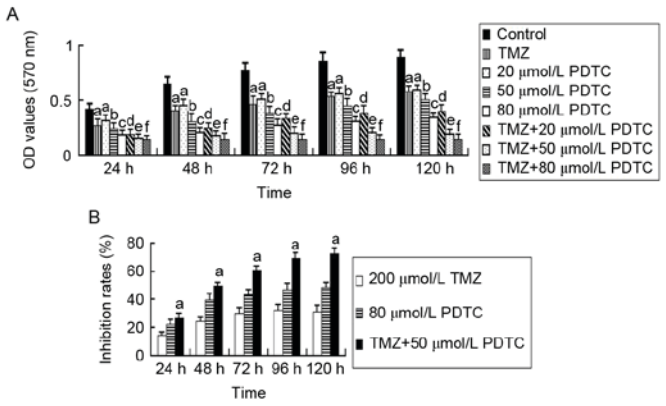

Figure 1. MTT assays detecting the viability of U251 cells treated with TMZ, PDTC and TMZ + PDTC. (A) OD values of cells in alternate groups. Cell OD values of PDTC groups were markedly lower than the control group and decreased with increasing PDTC concentrations (a: P<0.05, compared with the control group; b: P<0.05, compared with the control group and 20 μmol/l PDTC group; c: P<0.05, compared with the control group and 50 μmol/l PDTC group; independent-samples t test and one-way ANOVA followed by LSD analysis or Kruskal-Wallis test). Cell OD values of TMZ + PDTC groups were significantly lower than those of the TMZ group and the corresponding PDTC groups (d: P<0.05, compared with the TMZ group and 20 μmol/l PDTC group; e: P<0.05, compared with the TMZ group, 50 μmol/l PDTC group and TMZ + 20 μmol/l PDTC group; f: P<0.05, compared with TMZ group and 80 μmol/l PDTC group; one-way ANOVA followed by LSD analysis or the Kruskal-Wallis test). (B) Cell proliferation inhibition rates in three representative groups. The inhibition rates of the TMZ + 50 μmol/l PDTC treatment group were significantly higher, compared with 200 μmol/l TMZ or 80 μmol/l PDTC treatments at 24-120 h (a: P<0.05, compared with the TMZ and PDTC group, one-way ANOVA followed by LSD analysis). OD, optical density; TMZ, temozolomide; PDTC, pyrrolidine dithiocarbamate; ANOVA, analysis of variance; LSD, least significant difference.

variance (ANOVA) was used to analyze the significance among ≥3 groups and Fisher's least significant difference method for multiple comparisons was used when the probability for ANOVA was statistically significant. Methods of nonparametric statistical analysis including the Mann-Whitney U Test and Kruskal-Wallis ANOVA, were used when the variances did not pass the Levene test for normality or homogeneity. P<0.05 was considered to indicate a statistically significant difference.

Results

Combining TMZ and PDTC induces the highest proliferation inhibition rate. TMZ, PDTC and TMZ + PDTC treatments all significantly suppressed the proliferation of U251 cells (P<0.05). Cell OD values decreased with increasing PDTC concentrations (P<0.05; Fig. 1A). The TMZ and PDTC treatment combination exhibited a greater significant inhibiting effect and lower OD values compared with the corresponding PDTC group (P<0.05; TMZ + PDTC vs. PDTC). However, TMZ + 80 μmol/l PDTC did not induce lower OD values compared with TMZ + 50 μmol/l PDTC (P<0.05; Fig. 1A). The proliferation inhibition rates in the TMZ + PDTC 50 μmol/l PDTC group (61.56% at 72 h) were higher, compared with in the TMZ group (29.88% at 72 h) and 80 μmol/l PDTC group (44.02% at 72 h; P<0.05; Fig. 1B).

Combination of TMZ and PDTC induces the most significant cell apoptosis. Following an incubation of 24 h, TMZ, PDTC and TMZ + PDTC markedly induced cell apoptosis compared with the control (Fig. 2). TMZ + PDTC induced higher apoptosis rates as compared with TMZ and the corresponding concentrations of PDTC (Table III). The rate of cell apoptosis increased with increasing PDTC concentrations (P<0.05; Table III). However, when treated with 100 μmol/l PDTC or TMZ + ≥50 μmol/l PDTC, cell apoptosis rates reached >93%, and no significant difference had been identified among these groups (P<0.05; Table III).

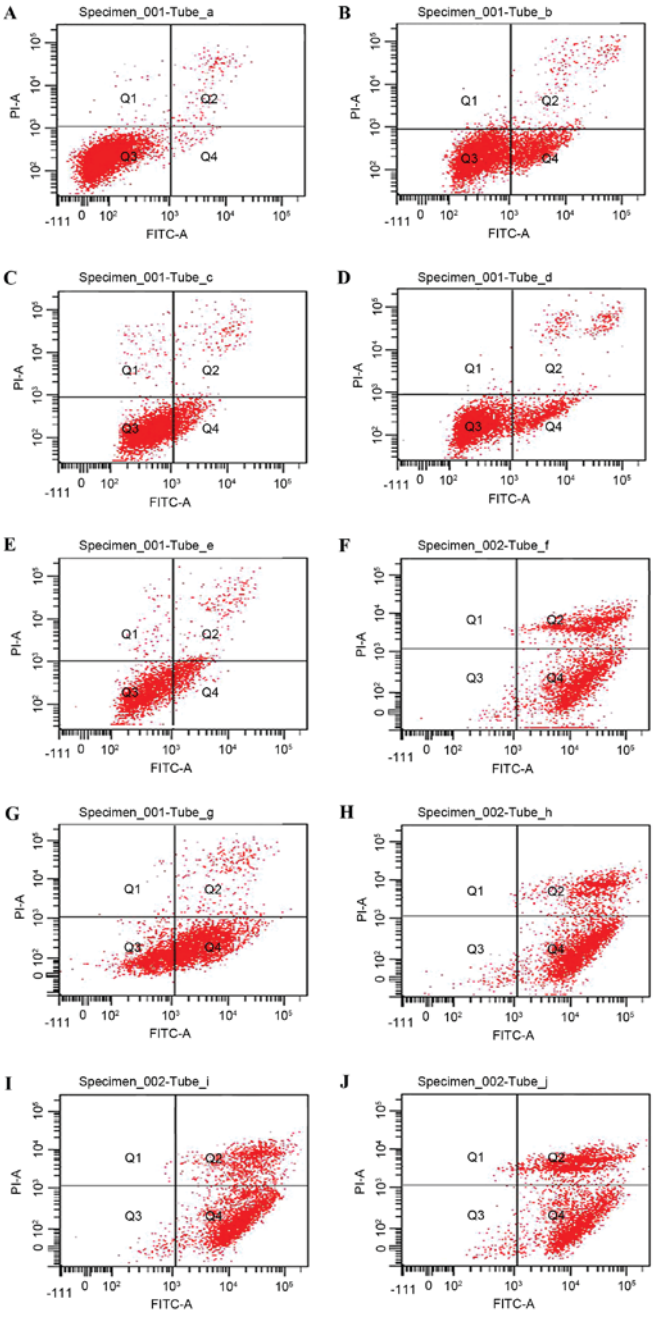

Figure 2. Flow cytometric analysis with Annexin V-FITC/PI staining detecting apoptosis of U251 cells in the control, TMZ, PDTC and TMZ + PDTC groups. (A) Control, (B) 200 μmol/l TMZ, (C) 20 μmol/l PDTC, (D) TMZ + 20 μmol/l PDTC, (E) 50 μmol/l PDTC, (F) TMZ + 50 μmol/l PDTC, (G) 80 μmol/l PDTC, (H) TMZ + 80 μmol/l PDTC, (I) 100 μmol/l PDTC and (J) TMZ + 100 μmol/l PDTC. FITC, fluorescein isothiocyanate; PI, propidium iodide; TMZ, temozolomide; PDTC, pyrrolidine dithiocarbamate.

Table III. Apoptosis rates of U251 cells in distinct groups.

Group	Concentration, μmol/l	Early stage, %	Late stage, %	Total apoptosis, %
Control		(1.6±0.54)	(0.8±0.03)	(2.4±1.03)
TMZ	200	(22.8±2.24)[a]	(3.1±0.75)[a]	(25.9±3.15)[a]
PDTC	20	(2.0±1.41)[a]	(2.7±0.43)[a]	(17.9±1.26)[a]
	50	(25.8±0.85)[b]	(5.8±0.91)[b]	(31.6±1.75)[b]
	80	(59.8±2.09)[c]	(4.1±1.46)	(63.9±4.24)[c]
	100	(71.7±2.76)[d]	(22.5±2.07)[d]	(93.2±4.73)[d]
TMZ + PDTC	20	(26.6±2.27)[e]	(6.7±0.85)[e]	(33.3±2.44)[e]
	50	(70.2±5.12)[f]	(21.5±2.57)[f]	(91.7±5.22)[f]
	80	(64.1±3.04)	(33.2±2.06)[g]	(97.3±4.46)[g]
	100	(57.7±3.55)	(39.2±2.89)[h]	(96.9±5.10)

Data were presented as the mean ± standard deviation. [a]P<0.05, vs. control group; [b]P<0.05, vs. control group and 20 μmol/l PDTC group; [c]P<0.05, vs. control group and 50 μmol/l PDTC group; [d]P<0.05, vs. control group and 80 μmol/l PDTC group; [e]P<0.05, vs. TMZ group and 20 μmol/l PDTC group; [f]P<0.05, vs. TMZ group, 50 μmol/l PDTC group and TMZ + 20 μmol/l PDTC group; [g]P<0.05, vs. TMZ group, 80 μmol/l PDTC group and TMZ + 50 μmol/l PDTC group; [h]P<0.05, vs. TMZ group, 100 μmol/l PDTC group and TMZ + 80 μmol/l PDTC group. All comparisons were carried out using one-way analysis of variance followed by least significant difference analysis or by the Kruskal-Wallis test. TMZ, temozolomide; PDTC, pyrrolidine dithiocarbamate.

PDTC enhances the cell cycle arresting effect of TMZ treatment. The combination of TMZ and PDTC led to a significant G_0/G_1 cell cycle arresting effect in U251 cells (Fig. 3). The percentage of cells in the G_0/G_1 stage in TMZ + PDTC groups was markedly higher than in the TMZ group (42.4±1.39%) and the corresponding PDTC groups (P<0.05), whereas the percentage of cells in the G_2 stage in TMZ + PDTC groups were markedly lower compared with that in the TMZ group (25.1±1.14%) and the corresponding PDTC groups (P<0.05; Table IV). A higher concentration of PDTC induced a higher proportion of cells in the G_0/G_1 stage; however, TMZ + 80 μmol/l PDTC induced no more significant G_0/G_1 arrest than TMZ + 50 μmol/l PDTC (P<0.05; Table IV).

PDTC suppresses the expression of MGMT, BCL-XL and survivin. Following incubation with PDTC for 48 h, the mRNA levels of *MGMT*, *BCL-XL* and *survivin* were significantly reduced (P<0.05; Fig. 4A-C). The protein levels of *MGMT*, *BCL-XL* and *survivin* were also reduced following PDTC treatment (Fig. 4D).

PDTC counteracts MGMT and BCL-XL upregulation induced by TMZ. *MGMT*, *BCL-XL* and *survivin* expression levels increased significantly, subsequent to TMZ treatment for 24 h (P<0.05; Fig. 5). However, this upregulation was abrogated by simultaneous treatment with PDTC. *MGMT* and *BCL-XL* expression levels in the PDTC + TMZ group were markedly lower compared with that in the TMZ group, whereas *survivin* expression was not altered significantly (P<0.05; Fig. 5).

Discussion

NF-κB serves a number of critical roles in the development, invasion, recurrence and chemoresistance of malignant brain glioma (30). Abnormal constitutive activation of the NF-κB signaling pathway may be identified in a large number of clinical glioma specimens (31). Wang *et al* (32) revealed that >90% of the 259 human diffuse gliomas included in the study exhibited high activation of NF-κB, and the extent of activation represented by the protein expression level of the p65 subunit was positively associated with glioma grade and malignancy. Highly activated NF-κB may lead to increased expression levels of matrix metalloproteinases (*MMPs*) (33) and vascular endothelial growth factor (*VEGF*), which facilitates microvascular invasion and distal metastases of glioblastoma stem cells (GSCs) (34). In conjunction with the high level of constitutive activity, it has previously been demonstrated that numerous alkylating agents may activate NF-κB in glioma cells (35). Contributing to the anti-apoptotic effect of the NF-κB signaling pathway and blocking constitutive or stimulated NF-κB activation may be a potential approach to suppressing glioma cell viability and enhance the efficacy of alkylating drugs (36).

Furthermore, the inhibition of NF-κB by genetic or chemical inhibitors induces apoptosis of various glioma cells and restores the apoptotic response following treatment with ionizing radiation or chemotherapeutic agents, thus reversing NF-κB linked radioresistance or chemoresistance in a number of models (37). For example, when NF-κB function was profoundly suppressed in U87 and U251 glioma cells via the overexpression of non-degradable IκB, chemical agents including carmustine (BCNU), carboplatin, SN38 glucuronide and tumor necrosis factor-α, induced significant proliferation inhibition and apoptosis in these refractory cell lines (29). SN50, a specific NF-κB inhibitor, may induce differentiation and reduce malignant characters (including neuro-sphere formation, motility, invasion and tumor initiation *in vivo*) of GSCs. The GSCs sensitivity to TMZ and radiotherapy was markedly enhanced by a low dose of SN50 (38). In the present study, another specific NF-κB inhibitor, PDTC, was used: PDTC is membrane permeable and an antioxidant (39). PDTC may reduce the phosphorylation and degradation of IκB and

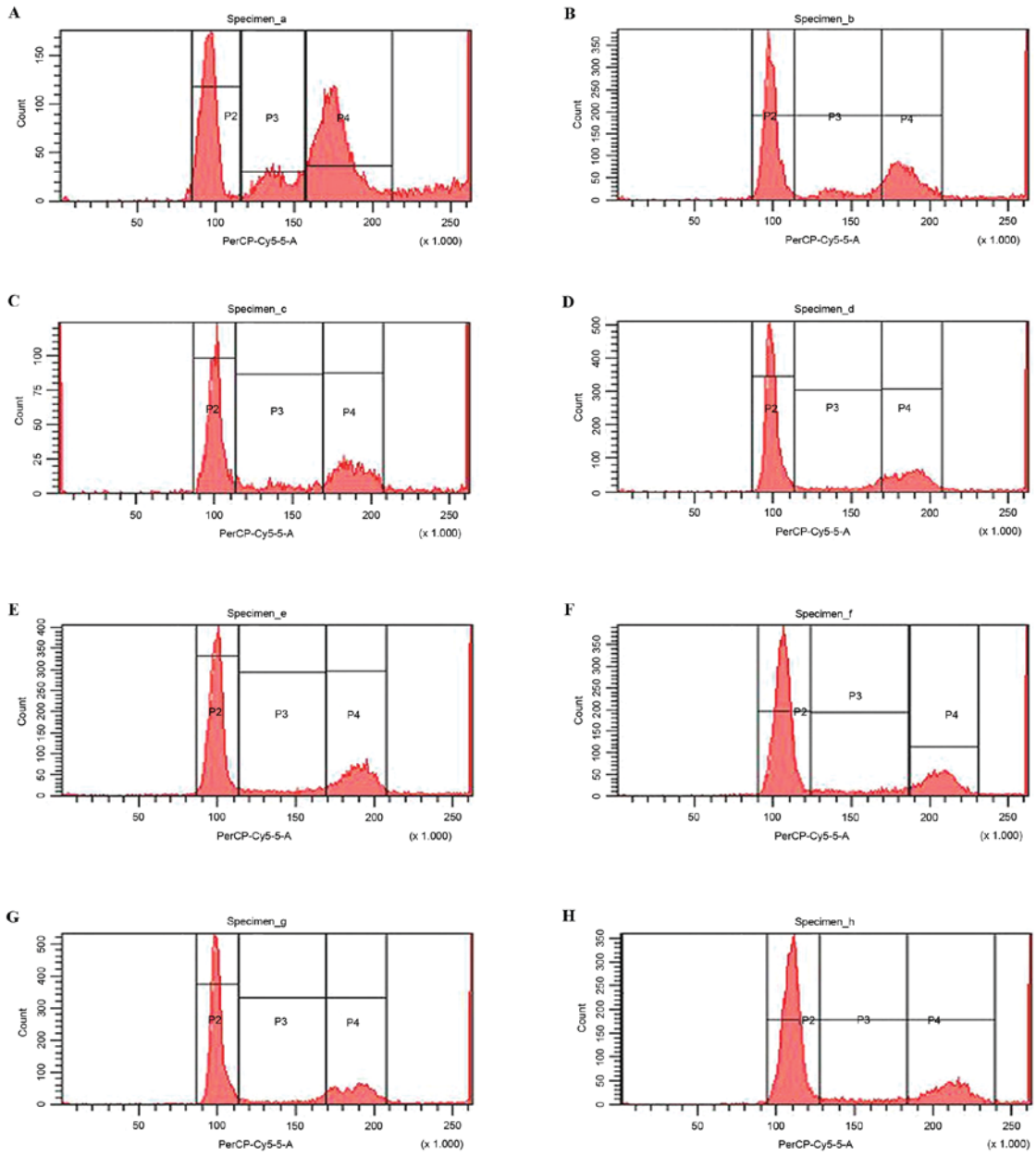

Figure 3. Flow cytometry analysis of U251 cells in G_0/G_1, S and G_2 phases following treatment with PDTC in various concentrations. (A) Control, (B) 200 μmol/l TMZ, (C) 20 μmol/l PDTC, (D) TMZ + 20 μmol/l PDTC, (E) 50 μmol/l PDTC, (F) TMZ + 50 μmol/l PDTC, (G) 80 μmol/l PDTC, (H) TMZ + 80 μmol/l PDTC. (P1) G_0/G_1 phase, (P2) S phase, (P3) G_2 phase. PDTC, pyrrolidine dithiocarbamate; TMZ, temozolomide.

subsequently block NF-κB activation and nuclear translocation (40). In conjunction with previous studies (28,41,42), the results of the MTT assay and flow cytometry conducted in the present study demonstrated that a low concentration of PDTC may markedly inhibit proliferation and induce apoptosis in U251 cells. Furthermore, the combined treatment of TMZ and PDTC led to a significant increase in proliferation-inhibition rate, apoptosis rate and a more significant cell cycle arrest, as compared with TMZ or PDTC treatment alone (Figs. 1-3). These results indicated a synergistic effect between TMZ and NF-κB inhibitors; a comprehensive understanding of the molecular mechanisms underlying this synergistic action may facilitate the exploration of more efficacious NF-κB inhibitors and a practical combination strategy of NF-κB inhibitors and alkylating agents.

As previously described, *MGMT* is a key factor of chemoresistance in gliomas (10) and inhibiting the NF-κB signaling pathway may markedly enhance TMZ chemotherapeutic efficacy in U251 cells (37). The results of current study suggest that NF-κB inhibitors mediate their killing effects by inhibiting a potential NF-κB/*MGMT* signaling pathway. In order to further support this suggestion, evidence is required which indicates that an NF-κB/*MGMT* signaling pathway exists in glioma cells and that NF-κB inhibitors, including PDTC, significantly reduce *MGMT* expression in glioma cell lines following treatment with alkylating agents. A number of studies have previously demonstrated the existence of an NF-κB/*MGMT* signaling pathway in glioma cells (15,43,44). Two putative NF-κB binding sites within the *MGMT* promoter region have been discovered by Lavon *et al* (28), demonstrated

Table IV. Cell cycle distribution of U251 cells in distinct groups.

Group	Concentration, μmol/l	G_0/G_1, %	S, %	G2, %
Control		(26.0±1.42)	(10.4±1.36)	(34.2±1.85)
TMZ	200	(42.4±1.39)[a]	(9.8±1.71)	(25.1±1.14)[a]
PDTC	20	(38.3±2.52)[a]	(9.5±1.83)	(21.5±0.94)[a]
	50	(47.7±3.32)[b]	(7.9±1.53)[b]	(21.6±3.04)
	80	(50.8±4.05)[c]	(6.8±1.32)	(21.3±2.16)
TMZ + PDTC	20	(49.1±4.02)[d]	(8.1±0.47)	(17.7±2.06)[d]
	50	(58.2±2.17)[e]	(7.8±1.42)	(16.7±3.22)
	80	(59.3±2.92)	(6.3±2.57)	(18.6±2.58)

Data are presented as the mean ± standard deviation. [a]P<0.05, vs. control group; [b]P<0.05 vs. control group and 20 µmol/l PDTC group; [c]P<0.05, vs. control group and 50 µmol/l PDTC group; [d]P<0.05, vs. TMZ group and 20 µmol/l PDTC group; [e]P<0.05, vs. control group, 50 µmol/l PDTC group and TMZ + 20 µmol/l PDTC group. All comparisons were carried out using one-way analysis of variance followed by least significant difference analysis or by the Kruskal-Wallis test. TMZ, temozolomide; PDTC, pyrrolidine dithiocarbamate.

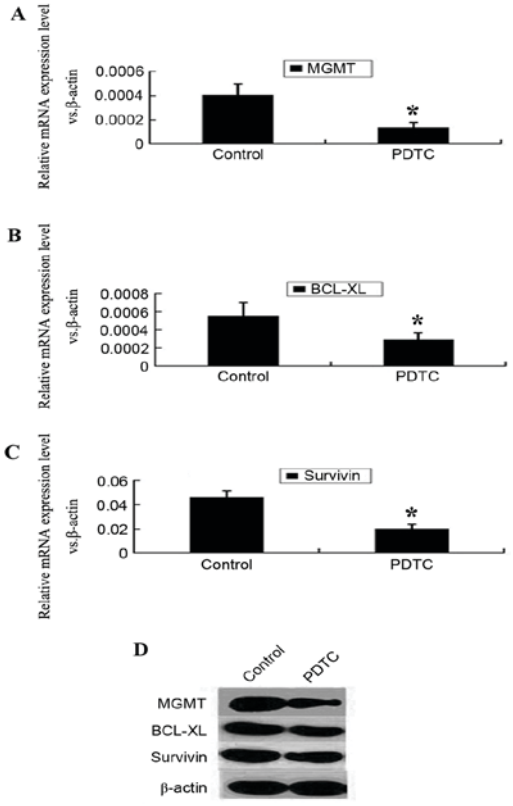

Figure 4. PDTC treatment suppresses *MGMT*, *BCL-XL* and *survivin* expression levels. (A) RT-qPCR results demonstrated that mRNA levels of *MGMT* were markedly decreased in PDTC-treated cells. (B) The *BCL-XL* mRNA level was significantly lower following PDTC treatment. (C) The mRNA level of *survivin* was also much lower in the PDTC group. *P<0.05 compared with control cells. (D) Western blotting results demonstrated lower *MGMT*, *BCL-XL* and *survivin* protein expression levels in the PDTC treated cells, compared with the control U251 cells. PDTC, pyrrolidine dithiocarbamate; *MGMT*, O-6-methylguanine-DNA methyltransferase; *BCL-XL*, B-cell lymphoma extra-large; RT-qPCR, reverse transcription-quantitative polymerase chain reaction.

a specific and direct interaction of NF-κB at each of these sites. They further revealed that forced expression of the NF-κB subunit p65 in HEK293 cells and glioma cells induced an increase in *MGMT* expression levels, whereas the addition of the NF-κB inhibitor IκB completely abrogated this induction (28). *MGMT* expression was revealed to be attenuated by fluoxetine via disrupting the NF-κB signaling pathway and consequently sensitized 98 G, SF767 and U251 glioma cells to TMZ treatment (44). Similarly, the present study identified markedly lower *MGMT* expression levels in PDTC-treated U251 cells (Fig. 4). As aforementioned, alkylating agents may activate the NF-κB signaling pathway, and NF-κB serves an important role in *MGMT* regulation. Also, it has previously been revealed that alkylating drugs stimulate *MGMT* expression in glioma cells (45). Therefore, an NF-κB/*MGMT* signaling pathway may be activated by alkylating drugs, in addition to stimulating *MGMT* expression. Other anti-apoptotic mechanisms may also serve major roles in NF-κB-mediated chemoresistance to alkylating agents (31). In order to confirm these suggestions, the present study treated U251 cells with 100 μmol/l TMZ. As a notable result, significant increases in *MGMT* expression levels and in two additional NF-κB downstream genes, *BCL-XL* and *survivin*, were demonstrated.

Additional evidence derives from a previous study by Lavon *et al* (28), which revealed that the suppression of *MGMT* activity with O6-benzylguanine eradicates the chemoresistance acquired by glioma cell lines, with ectopic p65 or high constitutive NF-κB activity. Despite the understanding that high *MGMT* expression in resistant glioma cells is stimulated by constitutive or drug-activated high NF-κB activity (29,32), evidence from previous studies supports the present study's hypothesis of the existence and the contribution of an NF-κB/*MGMT* signaling pathway towards chemoresistance (28,43,44). However, the questions remain about whether this signaling pathway may be exploited to combat fatal gliomas, and if the efficacy of combined TMZ and PDTC treatment is a result of the downregulation of *MGMT*. In order to investigate these considerations, the present study compared the expression levels of *MGMT* in cells treated with TMZ + PDTC and in cells treated with TMZ alone, it was revealed that the expression level of *MGMT* was significantly reduced by the addition of PDTC (Fig. 5). These results are supported by a number of similar previous studies (28,44). For

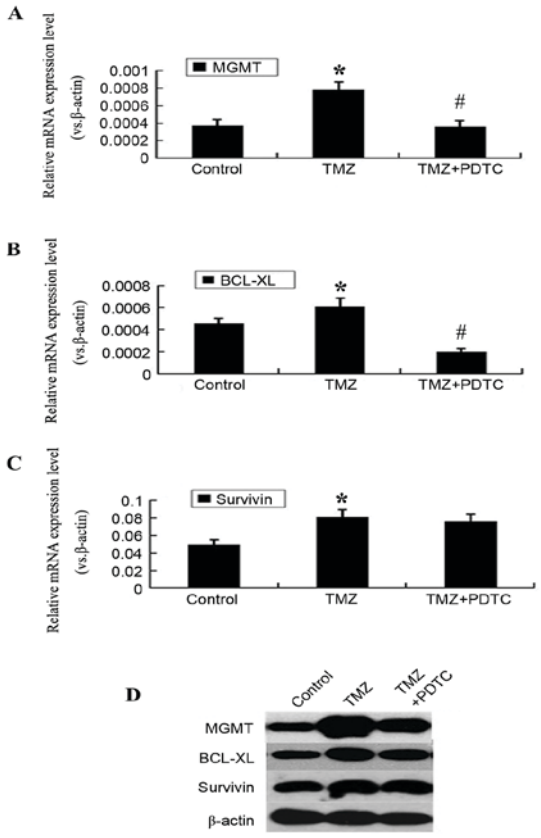

Figure 5. PDTC counteracts the upregulation of *MGMT* and *BCL-XL* induced by TMZ treatment. (A) RT-qPCR results revealed that mRNA level of *MGMT* in TMZ-treated cells was significantly higher than that in control cells and TMZ + PDTC-treated cells. *P<0.05 compared with control cells, $^{\#}$P<0.05 compared with TMZ-treated cells. (B) The mRNA level of *BCL-XL* in TMZ-treated cells was higher than that in control cells and TMZ + PDTC-treated cells. *P<0.05 compared with control cells, $^{\#}$P<0.05 compared with TMZ-treated cells. (C) The *survivin* mRNA level in TMZ-treated cells was much higher than that in control cells, but showed no statistical difference between TMZ-treated cells and TMZ + PDTC treated cells. *P<0.05 compared with control cells. (D) Western blotting results demonstrated that *MGMT*, *BCL-XL* and *survivin* protein levels in TMZ treated cells were higher compared with the control cells; *MGMT* and *BCL-XL* protein levels of TMZ + PDTC treated cells were low compared with TMZ treated cells; however, the *survivin* protein level between TMZ + PDTC treated and TMZ treated cells demonstrated no obvious difference. PDTC, pyrrolidine dithiocarbamate; *MGMT,* O-6-methylguanine-DNA methyltransferase; *BCL-XL*, B-cell lymphoma extra-large; TMZ, temozolomide; RT-qPCR, reverse transcription-quantitative polymerase chain reaction.

instance, in glioblastoma initial cells, resveratrol was identified to block *MGMT* upregulation induced by TMZ treatment via inhibiting NF-κB activation (15). Therefore, downregulation of the NF-κB/*MGMT* signaling pathway is a feasible strategy in order to overcome TMZ-resistance. For example, BAY 11-7082, a specific IκB kinase (IKK) inhibitor leading to the de-activation of the NF-κB signaling pathway, sensitized selected U251 TMZ-resistant cells (TR/U251) to TMZ treatment, resulting in substantial cell death (37). However, Bay 11-7082 may induce cell death independent from inhibiting the activation of the NF-κB signaling pathway (46), and this is the reason for the selection of PDTC, instead of Bay 11-7082 in the present study.

In addition to the regulation of *MGMT* expression, the impact of NF-κB activity on its canonical target genes, including *BCL-XL*, *survivin*, *BCL-2*, inhibitor of apoptosis 1/2 (*IAP1*/*IAP2)*, TNF receptor associated factor 1/2, *VEGF*, matrix metallopeptidase 9 (*MMP9)* and *cyclin D1*, are also worth further study for glioma therapy. *BCL-XL*, *BCL-2*, *survivin* and IAP1/IAP2 are key anti-apoptotic factors contributing to cell survival, and are closely associated with the progression and chemotherapy or radiotherapy resistance of various types of cancer (47-49). *BCL-XL* upregulation by signal transducer and activator of transcription 3, contributes to mutant Kirsten rat sarcoma-mediated apoptosis resistance in colorectal cancer (49). In a recent study with 117 ovarian epithelial neoplasms, *survivin* overexpression was identified in the majority of malignant cases and was associated with patient prognosis, indicating a crucial role in the development of epithelial ovarian neoplasms (50). Furthermore, it has previously been revealed that *survivin* expression may be upregulated by treatment in certain lymphoid or myeloid tumors (48). As a consequence, a large number of novel antagonist and inhibitors of these anti-apoptotic factors have been developed, and a number of them demonstrated good clinical results (47,51). The overexpression of these anti-apoptotic factors may be induced by highly activated upstream NF-κB; therefore, inhibiting NF-κB activity may be a potential method by which to suppress tumors with overexpressed *BCL-XL*, *BCL-2* or *survivin* (52). In conjunction, the present study identified that the expression of *BCL-XL* and *survivin* are significantly inhibited by PDTC treatment in U251 cells (Fig. 4). Furthermore, NF-κB activity and, consequently, *cyclin D1*, *COX-2*, *BCL-XL* and *BCL-2* expression levels may be suppressed *in vivo* in prostate tumors by Apigenin, which has been administrated to transgenic adenocarcinoma mouse prostates (53). Similarly, *MGMT*, *BCL-XL*, *BCL-2* and *survivin* serve important roles in NF-κB mediated therapeutic resistance (54). Conversely, combining traditional agents with novel inhibitors of these survival and anti-apoptotic factors may be a promising cancer therapy strategy (55). Downregulated anti-apoptotic factors may be an additional mechanism underlying PDTC-enhanced TMZ efficacy in the present study, particularly considering that NF-κB and its downstream anti-apoptotic factors are often stimulated by radiotherapy and chemotherapy (54). The present study also demonstrated TMZ induced the upregulation of *BCL-XL* and *survivin* in U251 cells. Additionally, a lower level of *BCL-XL*, not *survivin*, was demonstrated in PDTC + TMZ treated cells, as compared with TMZ only treated cells (Fig. 5). Therefore, a reduction *BCL-XL* expression may serve a role in PDTC induced U251 cell sensitivity to TMZ, whereas the expression level of *survivin* may not be altered significantly in TMZ treated cells by PDTC, at a low concentration of ~50 μmol/l.

The results of the present study in regards to *survivin* were in accordance with the findings of Elhag *et al* (56), which revealed that the ability of silibinin, a natural plant component, to potentiate the cytotoxic efficacy of TMZ in human LN229, U87 and A172 glioblastoma cells was unrelated to *survivin* protein levels, whereas silibilin may attenuate metastatic processes by suppressing NF-κB and the downstream gene, *MMP9*. Additionally, it was revealed that expression levels of *cyclin D1* were not significantly altered by PDTC treatment, although the addition of PDTC led to an enhanced G_0/G_1 phase arresting effect (56).

The present study demonstrated that PDTC, a widely tested inhibitor of NF-κB activation as well as an antioxidant

and metal chelator, may inhibit cell proliferation, induce apoptosis and cell cycle arrest and enhance sensitivity to TMZ in U251 glioma cells. It was also revealed that PDTC sensitized U251 cells to TMZ, mainly via blocking the NF-κB and NF-κB/*BCL-XL* signaling pathways that were activated by TMZ treatment. Currently, a large number of anti-NF-κB drugs have been developed for cancer therapy (57); the results of the present study may provide specific aid in furthering the understanding of the chemotherapeutic effects, and the underlying mechanisms involved in inhibiting NF-κB in glioma cells, thus providing an important theoretical basis for developing NF-κB inhibitors with greater efficacy and improved methods of cancer treatment.

Acknowledgements

The present study was supported by The National Natural Science Foundation of China (grant no. NSFC: 81272783) and The National Key Technology Research and Development Program of the Ministry of Science and Technology of China (grant no. 2014BAI04B02). The authors thank Mrs Xiaohong Yang (The National Institute of Biological Sciences, Beijing, China) for her contributions and Dr Weiliang Jiang (Shanghai Jiaotong University School of Medicine, Shanghai, China) for his comments on the manuscript.

References

1. Ohgaki H and Kleihues P: Epidemiology and etiology of gliomas. Acta Neuropathol 109: 93-108, 2005.
2. Louis DN, Perry A, Burger P, Ellison DW, Reifenberger G, von Deimling A, Aldape K, Brat D, Collins VP, Eberhart C, *et al*: International society of neuropathology-haarlem consensus guidelines for nervous system tumor classification and grading. Brain Pathol 24: 429-435, 2014.
3. Carlsson SK, Brothers SP and Wahlestedt C: Emerging treatment strategies for glioblastoma multiforme. EMBO Mol Med 6: 1359-1370, 2014.
4. Stupp R, Hegi ME, Mason WP, van den Bent MJ, Taphoorn MJ, Janzer RC, Ludwin SK, Allgeier A, Fisher B, Belanger K, *et al*: Effects of radiotherapy with concomitant and adjuvant temozolomide versus radiotherapy alone on survival in glioblastoma in a randomised phase III study: 5-year analysis of the EORTC-NCIC trial. Lancet Oncol 10: 459-466, 2009.
5. Gilbert MR, Friedman HS, Kuttesch JF, Prados MD, Olson JJ, Reaman GH and Zaknoen SL: A phase II study of temozolomide in patients with newly diagnosed supratentorial malignant glioma before radiation therapy. Neuro Oncol 4: 261-267, 2002.
6. Villano JL, Seery TE and Bressler LR: Temozolomide in malignant gliomas: Current use and future targets. Cancer Chemother Pharmacol 64: 647-655, 2009.
7. Roos WP, Batista LF, Naumann SC, Wick W, Weller M, Menck CF and Kaina B: Apoptosis in malignant glioma cells triggered by the temozolomide-induced DNA lesion O6-methylguanine. Oncogene 26: 186-197, 2007.
8. Jacinto FV and Esteller M: MGMT hypermethylation: A prognostic foe, a predictive friend. DNA Repair (Amst) 6: 1155-1160, 2007.
9. Spiegl-Kreinecker S, Pirker C, Filipits M, Lötsch D, Buchroithner J, Pichler J, Silye R, Weis S, Micksche M, Fischer J and Berger W: O6-Methylguanine DNA methyltransferase protein expression in tumor cells predicts outcome of temozolomide therapy in glioblastoma patients. Neuro Oncol 12: 28-36, 2010.
10. Bobola MS, Alnoor M, Chen JY, Kolstoe DD, Silbergeld DL, Rostomily RC, Blank A, Chamberlain MC and Silber JR: O6-methylguanine-DNA methyltransferase activity is associated with response to alkylating agent therapy and with MGMT promoter methylation in glioblastoma and anaplastic glioma. BBA Clin 3: 1-10, 2015.
11. Vlachostergios PJ, Hatzidaki E and Papandreou CN: MGMT repletion after treatment of glioblastoma cells with temozolomide and O6-benzylguanine implicates NFκB and mutant p53. Neurol Res 35: 879-882, 2013.
12. Bocangel D, Sengupta S, Mitra S and Bhakat KK: p53-mediated down-regulation of the human DNA repair gene O6-methylguanine-DNA methyltransferase (MGMT) via interaction with Sp1 transcription factor. Anticancer Res 29: 3741-3750, 2009.
13. Pyko IV, Nakada M, Sabit H, Teng L, Furuyama N, Hayashi Y, Kawakami K, Minamoto T, Fedulau AS and Hamada J: Glycogen synthase kinase 3β inhibition sensitizes human glioblastoma cells to temozolomide by affecting O6-methylguanine DNA methyltransferase promoter methylation via c-Myc signaling. Carcinogenesis 34: 2206-2217, 2013.
14. Okada M, Sato A, Shibuya K, Watanabe E, Seino S, Suzuki S, Seino M, Narita Y, Shibui S, Kayama T and Kitanaka C: JNK contributes to temozolomide resistance of stem-like glioblastoma cells via regulation of MGMT expression. Int J Oncol 44: 591-599, 2014.
15. Huang H, Lin H, Zhang X and Li J: Resveratrol reverses temozolomide resistance by downregulation of MGMT in T98G glioblastoma cells by the NF-κB-dependent pathway. Oncol Rep 27: 2050-2056, 2012.
16. Senftleben U and Karin M: The IKK/NF-kappaB pathway. Crit Care Med 30 (1 Supp): S18-S26, 2002.
17. Hayden MS and Ghosh S: Shared principles in NF-kappaB signaling. Cell 132: 344-362, 2008.
18. Hayden MS and Ghosh S: Regulation of NF-κB by TNF family cytokines. Semin Immunol 26: 253-266, 2014.
19. Rayet B and Gélinas C: Aberrant rel/nfkb genes and activity in human cancer. Oncogene 18: 6938-6947, 1999.
20. Karin M, Cao Y, Greten FR and Li ZW: NF-kappaB in cancer: From innocent bystander to major culprit. Nat Rev Cancer 2: 301-310, 2002.
21. Annunziata CM, Davis RE, Demchenko Y, Bellamy W, Gabrea A, Zhan F, Lenz G, Hanamura I, Wright G, Xiao W, *et al*: Frequent engagement of the classical and alternative NF-kappaB pathways by diverse genetic abnormalities in multiple myeloma. Cancer Cell 12: 115-130, 2007.
22. Cheng ZX, Sun B, Wang SJ, Gao Y, Zhang YM, Zhou HX, Jia G, Wang YW, Kong R, Pan SH, *et al*: Nuclear factor-κB-dependent epithelial to mesenchymal transition induced by HIF-1α activation in pancreatic cancer cells under hypoxic conditions. PLoS One 6: e23752, 2011.
23. Garner JM, Fan M, Yang CH, Du Z, Sims M, Davidoff AM and Pfeffer LM: Constitutive activation of signal transducer and activator of transcription 3 (STAT3) and nuclear factor κB signaling in glioblastoma cancer stem cells regulates the Notch pathway. J Biol Chem 288: 26167-26176, 2013.
24. Huber MA, Azoitei N, Baumann B, Grünert S, Sommer A, Pehamberger H, Kraut N, Beug H and Wirth T: NF-kappaB is essential for epithelial-mesenchymal transition and metastasis in a model of breast cancer progression. J Clin Invest 114: 569-581, 2004.
25. Cheng ZX, Wang DW, Liu T, Liu WX, Xia WB, Xu J, Zhang YH, Qu YK, Guo LQ, Ding L, *et al*: Effects of the HIF-1α and NF-κB loop on epithelial-mesenchymal transition and chemoresistance induced by hypoxia in pancreatic cancer cells. Oncol Rep 31: 1891-1898, 2014.
26. Puliyappadamba VT, Hatanpaa KJ, Chakraborty S and Habib AA: The role of NF-kappaB in the pathogenesis of glioma. Mol Cell Oncol 1: e963478, 2014.
27. Caporali S, Levati L, Graziani G, Muzi A, Atzori MG, Bonmassar E, Palmieri G, Ascierto PA and D'Atri S: NF-κB is activated in response to temozolomide in an AKT-dependent manner and confers protection against the growth suppressive effect of the drug. J Transl Med 10: 252, 2012.
28. Lavon I, Fuchs D, Zrihan D, Efroni G, Zelikovitch B, Fellig Y and Siegal T: Novel mechanism whereby nuclear factor kappaB mediates DNA damage repair through regulation of O(6)-methylguanine-DNA-methyltransferase. Cancer Res 67: 8952-8959, 2007.
29. Weaver KD, Yeyeodu S, Cusack JC Jr, Baldwin AS Jr and Ewend MG: Potentiation of chemotherapeutic agents following antagonism of nuclear factor kappa B in human gliomas. J Neurooncol 61: 187-196, 2003.
30. Lee DW, Ramakrishnan D, Valenta J, Parney IF, Bayless KJ and Sitcheran R: The NF-κB RelB protein is an oncogenic driver of mesenchymal glioma. PLoS One 8: e57489, 2013.

31. Wang L, Wei B, Hu G, Wang L, Bi M, Sun Z and Jin Y: Screening of differentially expressed genes associated with human glioblastoma and functional analysis using a DNA microarray. Mol Med Rep 12: 1991-1996, 2015.
32. Wang H, Wang H, Zhang W, Huang HJ, Liao WS and Fuller GN: Analysis of the activation status of Akt, NFkappaB, and Stat3 in human diffuse gliomas. Lab Invest 84: 941-951, 2004.
33. Sun P, Mu Y and Zhang S: A novel NF-κB/MMP-3 signal pathway involves in the aggressivity of glioma promoted by Bmi-1. Tumour Biol 35: 12721-12727, 2014.
34. Wang Z, Banerjee S, Li Y, Rahman KM, Zhang Y and Sarkar FH: Down-regulation of notch-1 inhibits invasion by inactivation of nuclear factor-kappaB, vascular endothelial growth factor, and matrix metalloproteinase-9 in pancreatic cancer cells. Cancer Res 66: 2778-2784, 2006.
35. Wang CY, Cusack JC Jr, Liu R and Baldwin AS Jr: Control of inducible chemoresistance: Enhanced anti-tumor therapy through increased apoptosis by inhibition of NF-kappaB. Nat Med 5: 412-417, 1999.
36. Kim HJ, Hawke N and Baldwin AS: NF-kappaB and IKK as therapeutic targets in cancer. Cell Death Differ 13: 738-747, 2006.
37. Wang X, Jia L, Jin X, Liu Q, Cao W, Gao X, Yang M and Sun B: NF-κB inhibitor reverses temozolomide resistance in human glioma TR/U251 cells. Oncol Lett 9: 2586-2590, 2015.
38. Zhang L, Ren X, Cheng Y, Liu X, Allen JE, Zhang Y, Yuan Y, Huang SY, Yang W, Berg A, *et al*: The NFκB inhibitor, SN50, induces differentiation of glioma stem cells and suppresses their oncogenic phenotype. Cancer Biol Ther 15: 602-611, 2014.
39. Qin JD, Cao ZH, Li XF, Kang XL, Xue Y, Li YL, Zhang D, Liu XY and Xue YZ: Effect of ammonium pyrrolidine dithiocarbamate (PDTC) on NF-κB activation and CYP2E1 content of rats with immunological liver injury. Pharm Biol 52: 1460-1466, 2014.
40. Kan S, Zhou H, Jin C and Yang H: Effects of PDTC on NF-κB expression and apoptosis in rats with severe acute pancreatitis-associated lung injury. Int J Clin Exp Med 8: 3258-3270, 2015.
41. Zhang JJ, Xu ZM, Zhang CM, Dai HY, Ji XQ, Wang XF and Li C: Pyrrolidine dithiocarbamate inhibits nuclear factor-κB pathway activation, and regulates adhesion, migration, invasion and apoptosis of endometriotic stromal cells. Mol Hum Reprod 17: 175-181, 2011.
42. Gu JW, Young E, Busby B, Covington J and Johnson JW: Oral administration of pyrrolidine dithiocarbamate (PDTC) inhibits VEGF expression, tumor angiogenesis, and growth of breast cancer in female mice. Cancer Biol Ther 8: 514-521, 2009.
43. Lan F, Yang Y, Han J, Wu Q, Yu H and Yue X: Sulforaphane reverses chemo-resistance to temozolomide in glioblastoma cells by NF-κB-dependent pathway downregulating MGMT expression. Int J Oncol 48: 559-568, 2016.
44. Song T, Li H, Tian Z, Xu C, Liu J and Guo Y: Disruption of NF-κB signaling by fluoxetine attenuates MGMT expression in glioma cells. Onco Targets Ther 8: 2199-2208, 2015.
45. Fritz G, Tano K, Mitra S and Kaina B: Inducibility of the DNA repair gene encoding O6-methylguanine-DNA methyltransferase in mammalian cells by DNA-damaging treatments. Mol Cell Biol 11: 4660-4668, 1991.
46. Rauert-Wunderlich H, Siegmund D, Maier E, Giner T, Bargou RC, Wajant H and Stühmer T: The IKK inhibitor Bay 11-7082 induces cell death independent from inhibition of activation of NFκB transcription factors. PLoS One 8: e59292, 2013.
47. Opferman JT: Attacking cancer's Achilles heel: Antagonism of anti-apoptotic BCL-2 family members. FEBS J 283: 2661-2675, 2016.
48. Wall NR, Beck FW, Al-Katib AM and Mohammad RM: Treatment-induced expression of anti-apoptotic proteins in WSU-CLL, a human chronic lymphocytic leukemia cell line. J Drug Target 9: 329-339, 2001.
49. Zaanan A , Okamoto K, Kawakami H, Khazaie K, Huang S and Sinicrope FA: The mutant KRAS Gene Up-regulates BCL-XL protein via STAT3 to confer apoptosis resistance that is reversed by BIM protein induction and BCL-XL antagonism. J Biol Chem 290: 23838-23849, 2015.
50. Plewka D, Jakubiec-Bartnik B, Morek M, Bogunia E, Bienioszek M, Wolski H, Kotrych D, Dziekan K, Seremak-Mrozikiewicz A and Plewka A: Survivin in ovary tumors. Ginekol Pol 86: 525-530, 2015.
51. Zhou W, Xu J, Gelston E, Wu X, Zou Z, Wang B, Zeng Y, Wang H, Liu A, Xu L and Liu Q: Inhibition of Bcl-xL overcomes polyploidy resistance and leads to apoptotic cell death in acute myeloid leukemia cells. Oncotarget 6: 21557-21571, 2015.
52. Vallianou NG, Evangelopoulos A, Schizas N and Kazazis C: Potential anticancer properties and mechanisms of action of curcumin. Anticancer Res 35: 645-651, 2015.
53. Shukla S, Shankar E, Fu P, MacLennan GT and Gupta S: Suppression of NF-κB and NF-κB-regulated gene expression by apigenin through IκBα and IKK pathway in TRAMP mice. PLoS One 10: e0138710, 2015.
54. Bravatà V, Minafra L, Russo G, Forte GI, Cammarata FP, Ripamonti M, Casarino C, Augello G, Costantini F, Barbieri G, *et al*: High-dose ionizing radiation regulates gene expression changes in the MCF7 breast cancer cell line. Anticancer Res 35: 2577-2591, 2015.
55. Kunami N, Katsuya H, Nogami R, Ishitsuka K and Tamura K: Promise of combining a Bcl-2 family inhibitor with bortezomib or SAHA for adult T-cell leukemia/lymphoma. Anticancer Res 34: 5287-5294, 2014.
56. Elhag R, Mazzio EA and Soliman KF: The effect of silibinin in enhancing toxicity of temozolomide and etoposide in p53 and PTEN-mutated resistant glioma cell lines. Anticancer Res 35: 1263-1269, 2015.
57. Olivier S, Robe P and Bours V: Can NF-kappaB be a target for novel and efficient anti-cancer agents? Biochem Pharmacol 72: 1054-1068, 2006.